Proc. Natl. Acad. Sci. USA
Vol. 95, pp. 4772–4777, April 1998
Plant Biology, Biochemistry

Architectural specificity in chromatin structure at the TATA box *in vivo*: Nucleosome displacement upon β-phaseolin gene activation

GUOFU LI*, SIMON P. CHANDLER†, ALAN P. WOLFFE†, AND TIMOTHY C. HALL*‡

*Institute of Developmental and Molecular Biology and Department of Biology, Texas A&M University, College Station, TX 77843-3155; and †Laboratory of Molecular Embryology, National Institute of Child Health and Human Development, National Institutes of Health, Bethesda, MD 20892-5431

Edited by Mary-Dell Chilton, Novartis Seeds, Inc., Research Triangle Park, NC, and approved February 12, 1998 (received for review September 12, 1997)

ABSTRACT **Extensive studies of the β-phaseolin (*phas*) gene in transgenic tobacco have shown that it is highly active during seed embryogenesis but is completely silent in leaf and other vegetative tissues. *In vivo* footprinting revealed that the lack of even basal transcriptional activity in vegetative tissues is associated with the presence of a nucleosome that is rotationally positioned with base pair precision over three phased TATA boxes present in the *phas* promoter. Positioning is sequence-dependent because an identical rotational setting is obtained upon nucleosome reconstitution *in vitro*. A comparison of DNase I and dimethyl sulfate footprints *in vivo* and *in vitro* strongly suggests that this repressive chromatin architecture is remodeled concomitant with gene activation in the developing seed. This leads to the disruption of histone-mediated DNA wrapping and the assembly of the TATA boxes into a transcriptionally competent nucleoprotein complex.**

Chromatin structure is known to regulate expression from several animal and yeast genes, and evidence that precisely positioned nucleosomes serve as general repressors of transcription has been obtained *in vivo* and *in vitro* (1–4). Precise positioning of nucleosomes on DNA is a complex process that can be governed by the primary sequence (5, 6). Whereas most positioned nucleosomes are remodeled before, or concurrent with, transcriptional activation, the nucleosome over the TATA region must be displaced to permit formation of an initiation complex, possibly through exchange with TFIID (7, 8). Evidence supporting this exchange includes recent biochemical and crystallographic evidence for a histone octamer-like substructure in TFIID (9–11). Additionally, the 10-bp repeat pattern of DNase I cleavage and protection in the adenovirus major late promoter region, which is protected by TFIID (12, 13), is similar to that obtained for nucleosomes (14) and is indicative of DNA lying on the surface of a protein complex.

In plants, the rapid accumulation of storage proteins during embryogenesis and seed development requires high transcriptional and translational activity. In contrast, promoters for seed storage protein genes are inactive in vegetative tissues. The spatial regulation of the promoter for β-phaseolin (*phas*), one of eight related genes encoding the major storage protein of bean (*Phaseolus vulgaris*) seed, is exceptionally tight both in bean and in transgenic tobacco (15–17). This is exemplified by the contrasting results for nuclear run-on transcription and β-glucuronidase (GUS) product accumulation shown in Fig. 1 for developing seeds and leaf tissues of tobacco transgenic for a *−1470phas/uidA* chimeric construct (17). The absolute constraint on expression from *phas* in vegetative tissues was demonstrated previously in tobacco transformed with *phas/DT-A* (diphtheria toxin A-chain) constructs. Although a single molecule per cell of DT-A is lethal, phenotypically normal plants were obtained (reflecting the complete absence of DT-A expression) (18). Initial zygotic development was normal, but embryos died on reaching the heart stage (5 to 10 days after pollination), consistent with activation of expression from the *phas* promoter. These differences in spatial expression could be attributed to the absence of suitable transcription factors specific for the *phas* gene in vegetative tissues. However, transient assays for GUS expression revealed substantial transcriptional activity from identical *phas* promoter constructs fused to the *uidA* reporter gene when introduced into leaf cells by bombardment or electroporation, showing that nuclear factors capable of interacting productively with *phas* promoter elements are present in vegetative tissues (19). The dramatic difference in expression from similar promoter constructs when stably integrated into the genome or supplied as naked DNA strongly suggested the involvement of chromatin as a major regulatory factor.

Here, we describe the use of both *in vivo* and *in vitro* approaches to explore the possible involvement of chromatin architecture in *phas* gene regulation. Our results show that a nucleosome rotationally positioned over the TATA region of the *phas* promoter is responsible for the absence of *phas* gene expression in leaf tissue. This rotationally positioned nucleosome is, however, disrupted in transcriptionally active seed tissues. Our data provide *in vivo* evidence that changes in the architecture of the TATA region of the *phas* promoter during transcriptional activation involve replacement of a histone octamer by the nucleosome-like substructure within TFIID. The possibility that phased TATA boxes serve as a rotational signal for nucleosome positioning is also discussed.

MATERIALS AND METHODS

Histochemical GUS Staining. Leaves or embryos (dissected from mid-maturation seeds) from tobacco transgenic for *−1470phas/uidA* (17) were incubated in Petri dishes with reaction buffer (1.5 mM 5-bromo-4-chloro-3-indolyl-β-D-glucuronide/1.5 mM potassium ferricyanide/1.5 mM potassium ferrocyanide/0.1 M $NaPO_4$, pH 7.0/10 mM EDTA/0.2% Triton) at 37°C for 16 hr. Chlorophyll was removed by using ethanol.

Nuclei Isolation. Tissue was powdered in a mortar and pestle by using liquid nitrogen, then treated with nuclei isolation buffer NIB1 [0.5 M hexylene glycol/20 mM KCl/20 mM Pipes, pH 6.5/0.5 mM EDTA/0.4% Triton X-100/0.05 mM spermine/0.125 mM spermidine/7 mM 2-mercaptoethanol/0.5 mM phenylmethylsulfonyl fluoride/0.5% (vol/vol) Aprotonin; Sigma]. The extract was filtered sequentially through 500-, 250-, 80-, 45-, and 20-μm mesh sieves and loaded onto a 20–80% Percoll (Sigma) step gradient. For leaves, chloroplasts re-

The publication costs of this article were defrayed in part by page charge payment. This article must therefore be hereby marked "*advertisement*" in accordance with 18 U.S.C. §1734 solely to indicate this fact.

This paper was submitted directly (Track II) to the *Proceedings* office.
Abbreviations: DMS, dimethyl sulfate; LMPCR, ligation-mediated PCR; *phas*, phaseolin gene; TBP, TATA-binding protein; *uidA*, the gene encoding β-glucuronidase (GUS).
‡To whom reprint requests should be addressed. e-mail: tim@bio.tamu.edu.

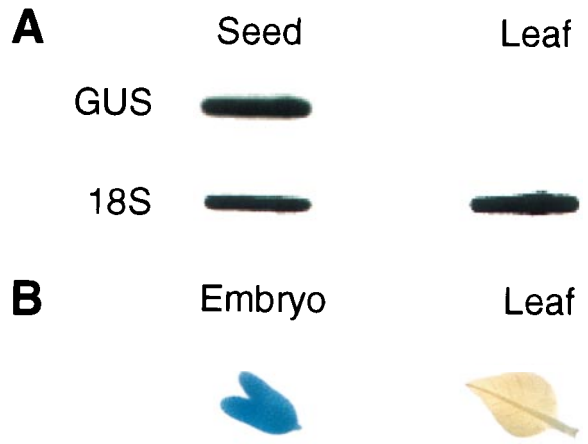

FIG. 1. The *phas* promoter drives expression in seed embryo but not in leaf tissue. (*A*) Transcriptional activity detected by run-on analysis using nuclei from mid-maturation embryos or leaves from a tobacco plant containing a single copy of −1470*phas*/*uidA*. Labeled run-on RNA was hybridized to a slot blot containing plasmid DNA encoding GUS or 18S ribosomal RNA. (*B*) Histochemical staining of a representative seed embryo and a leaf from the plant used in *A*. Blue color reveals accumulated GUS protein.

mained in the top layer whereas for seeds, starch grains pelleted through the 80% Percoll layer. Nuclei were removed from the 20–80% Percoll interface, washed in NIB2 (NIB1 without Triton X-100), and stained with acridine orange for analysis under a microscope. We have found that using Pipes, pH 6.5, in place of Hepes, pH 7.4 (20), dramatically improved the quality of the nuclei and routinely yielded 4×10^7 nuclei from 5 g of leaf tissue and 5×10^7 nuclei from 4 g of immature seeds (obtained from 40 seed pods).

Nuclei Run-On Transcription Assay. Run-on transcription was performed essentially as described (21). Slot blots were prepared by using 0.45-mM nitrocellulose membranes (Schleicher & Schuell) containing 1 μg of linearized plasmid DNA. After hybridization, the filters were washed (final stringency, 0.1× SSC, 65°C) and analyzed on a FUJIX BAS 2000 Bio-Imaging Analyzer (FUJIX, Tokyo).

Ligation-Mediated PCR (LMPCR). LMPCR was done according to Mueller and Wold (22) with the following modification. After ligation of the linker and ethanol precipitation, DNA was dissolved in 85 μl of H_2O. Subsequently, 10 μl of 10× PCR buffer (10 mM Tris·HCl, pH 8.0/50 mM KCl/1.5 mM $MgCl_2$/0.01% gelatin/2 mM of each dNTP and 0.1% Triton X-100), 20 pmol of gene-specific primer P2, 20 pmol of linker primer, and 2.5 units of *Taq* polymerase were added. Samples were overlaid with 70 μl of mineral oil and amplified by 20 cycles of PCR. Primer extension was done by using *Taq* polymerase and γ-^{32}P-radiolabeled gene-specific primer 3. After precipitation, the DNA was dissolved in 20 μl loading buffer and nick sites were visualized by denaturing gel electrophoresis of 2- to 5-μl samples and analyzed on a FUJIX BAS 2000 Bio-Imaging Analyzer. The following sets of primers were used for LMPCR: (*i*) top strand, set 1, 5′-ACAGGACGTAACATAAGGGACTGAC-3′, 5′-GGACTGACCGTACCCACTCTGGATG-3′, and 5′-CGTACCCACTCTGGATGGATGGATGATG-3′; set 2, 5′-GCCCGGCTTTCTTGTAACGC-3′, 5′-TTCCACAGTTTTCGCGATCCAGAC-3′, and 5′-CCACAGTTTTCGCGATCCAGACTGAATGC-3′; (*ii*) bottom strand, 5′-CTCTTCCGCCACCTCAATTTC-3′, 5′-CTTCACTTCAACACACGTCAACCTGC-3′, and 5′-CAACACACGTCAACCTGCATATGCGTGTC-3′. All primers were gel-purified before use in LMPCR.

Nucleosome Reconstitution. The *phas* promoter, from position −1471 to +112, was cloned into pBluescript II (Stratagene). The fragment of interest was prepared by cleavage of the plasmid with *Afl*III at position −112, and with *Xba*I at +141 downstream from the +1 start site. Core histones were purified from chicken erythrocytes (23). Histone H1 was not present in the reconstitution reaction. These purified core histones were used together with DNA to reconstitute nucleosome cores by salt dialysis (24). Nucleosome cores reconstituted in this way were used for the mapping of translational positioning of histone–DNA contacts, i.e., where the histone octamer begins and ends association with a DNA sequence. This procedure is necessary because a pure population of DNA fragments is required to carry out the end-labeling step needed to determine fragment size (25). All other nucleosome core reconstitution experiments used the exchange procedure (26) where 0.5 μg of DNA was resuspended in 10 μl of TE, plus 10 mM 2-mercaptoethanol, 1 M NaCl, and 2.4 μg nucleosome cores. This was incubated at room temperature for 30 min, after which 5 μl TE was added at 15-min intervals for four additions. Fifteen minutes after the fourth addition, 170 μl of TE was added to complete the exchange.

TATA-Binding Protein (TBP), TFIIA, and TFIID Production and Purification. *Saccharomyces cerevisiae* TBP and TFIIA (large and small subunits) were expressed in *Escherichia coli* and purified as described in detail by Godde *et al.* (27). TFIID was purified (28) by using FLAG epitope-tagged TBP from the HeLa-derived cell line 3–10. The functionality of TFIID in transcription experiments was demonstrated by complementation in transcription reactions using other purified basal transcription factors (29).

TFIID-Binding Assay. The *Afl*III-*Xba*I fragment of the *phas* promoter construct in pBluescript II was end-labeled at the *Afl*III site by cleavage with *Afl*III, followed by the addition of DNA polymerase I (pol I) Klenow fragment and radiolabeled dNTPs. Finally, after cleavage with *Xba*I, the fragment was purified on an acrylamide gel (30). The labeled *Afl*III-*Xba*I fragment (50 ng) was mixed with purified TFIID in binding buffer (50 mM Hepes-NaOH, pH7.9/8% glycerol/4 mM $MgCl_2$/60 mM KCl/5 mM DTT/0.2 mM EDTA/0.05% Nonidet P-40) (28), and, after equilibration at room temperature for 30 min, the complex was cleaved by hydroxyl radicals generated by the Fenton reaction (31) and the products were separated on a 6% denaturing gel.

RESULTS AND DISCUSSION

A Nucleosome Is Rotationally Positioned on the TATA Region of the Inactive but Not the Active *phas* Promoter. DNase I mapping *in vivo* of both the top (Fig. 2*A*, lanes 5 and 6) and bottom (data not shown) strands of the TATA region of the transcriptionally inactive *phas* promoter in leaf tissue revealed a 10-bp repeat pattern of cleavage sites interspersed with protected bases. The cuts on the two strands are staggered by 2–4 bp, characteristic for a DNA double helix wrapped around a protein surface. The 10-bp repeat extends for more than 140 bp, suggesting that a nucleosome is positioned over the TATA box and initiator regions of the inactive *phas* promoter. Although the pattern for *in vivo* DNase I footprinting of the *phas* promoter in seed nuclei (Fig. 2*A*, lanes 1 and 2) reveals a 10-bp repeat, the profile is different from that in leaf tissue. First, cutting at hypersensitive sites in the *phas* initiator region in seed nuclei is stronger than that in leaf nuclei. Second, the accessibility of adjacent nucleotides to cleavage appears to be much greater in seed than in leaf nuclei. An important third difference is the extent of the 10-bp cleavage repeat, which is from −11 to +50 in seed tissue but from −93 to +70 in leaf tissue (Fig. 2). We suggest that precise chromatin structures are remodeled concomitant with tissue-specific gene activation. Additional evidence supporting our belief that the nucleosome is displaced on transcriptional activation is provided by DNase I and DMS footprinting seen *in vivo* at the three TATA boxes, the TTTCATCAT initiation site, and sites downstream of the transcription start site in seed

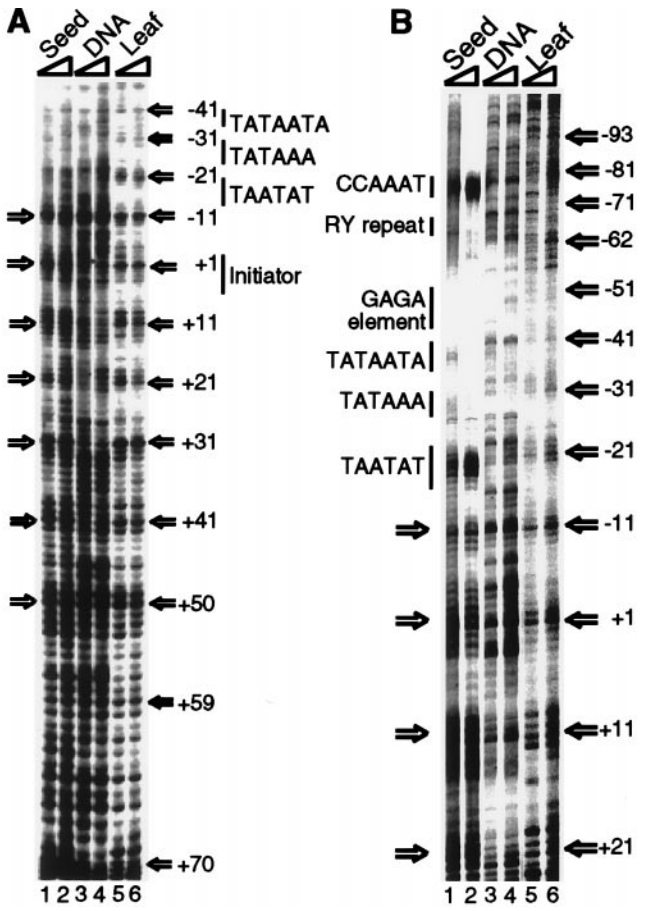

FIG. 2. DNase I footprinting *in vivo* of the top strand of the *phas* promoter proximal region. Nuclei were isolated from seed or leaf tissue and treated with various levels of DNase I. DNA was then extracted and subjected to LMPCR. (*A*) DNase I footprinting of the +70 to −41 *phas* promoter region from seed nuclei (lanes 1 and 2) and leaf nuclei (lanes 5 and 6) with naked DNA as a reference (lanes 3 and 4), using primers annealed to the +90 region. The DNase I concentrations used were: lane 1, 6 units; lane 2, 12 units; lane 3, 1 unit; lane 4, 2 units; lane 5, 6 units; lane 6, 12 units. (*B*) DNase I footprinting of the +21 to −93 region of the *phas* promoter in seed nuclei (lanes 1 and 2) and leaf nuclei (lanes 5 and 6) with naked DNA as a control (lanes 3 and 4), using primers annealed to the +45 region. DNase I concentrations used were as in *A*. For both *A* and *B*, open arrows show DNase I sensitivity at intervals of 10 bp, a pattern characteristic of DNA wrapped around a nucleosome or TFIID. Base positions are numbered relative to the transcription start site, and potentially important cis-elements are labeled.

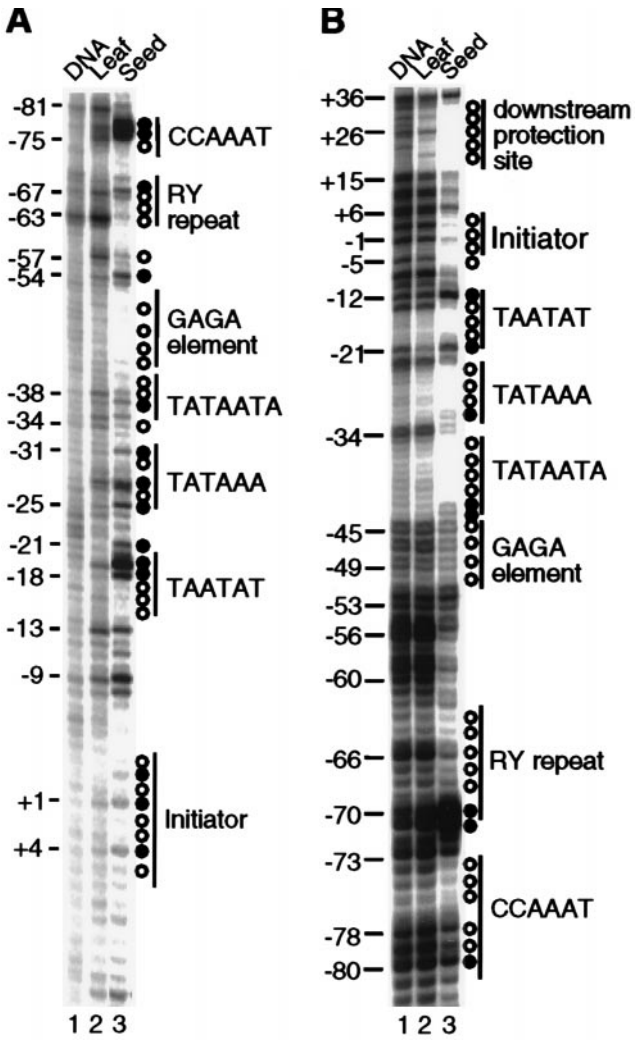

FIG. 3. DMS footprinting *in vivo* reveals factor binding to the active but not the inactive *phas* proximal promoter. Intact seeds or leaves of tobacco transformed with *phas-uidA* were treated with DMS. DNA was extracted and treated with piperidine (DMS and piperidine-treated genomic DNA was used as a control), and LMPCR analysis of the indicated regions of the *phas* promoter (relative to the transcription start site) was conducted by using appropriate primers. (*A*) Top strand. (*B*) Bottom strand. Consensus cis-element sites are indicated together with protected residues (open circles) and hypersensitive residues (solid circles).

tissues (Figs. 2 and 3). Factor binding to regions upstream of the TATA boxes in the transcriptionally active *phas* promoter differs from that for the inactive promoter. In vegetative tissue, over the 146-bp region where a nucleosome appears to be positioned, no obvious footprints were detected. Although there are some regions of hypersensitivity on the top strand that may be indicative of protein interaction (Fig. 3*A*), the almost identical footprinting pattern between naked DNA and leaf tissues on the bottom strand (Fig. 3*B*) does not support the existence of tight factor binding. Nevertheless, the lack of footprints in the DMS analysis of the bottom strand does not rule out the possibility of loose binding by nonhistone proteins because some hypersensitive sites (near −62, −81, and −93, Fig. 2*B*), and a protected site (−41, Fig. 2*B*), were detected for DNase I footprinting *in vivo*. Nevertheless, these observations may reflect variations in DNase I cleavage (32). In contrast, in seed tissue, an array of transcription factors clearly interacts with the region upstream of the TATA boxes. This is shown by the footprinting pattern over the CCAAAT box, the RY repeats, and the GAGA element (Fig. 3), which is similar to the profile obtained by DNase I footprinting *in vivo* (Fig. 2*B*).

Nucleosome Positioning on the TATA Region of the *phas* Promoter Is Sequence-Dependent. Nucleosomes were reconstituted *in vitro* on the *phas* proximal promoter region to test the structural consequence of histone association and to determine whether the primary sequence of the *phas* gene governed the observed rotational positioning. When these nucleosomes were subjected to DNase I treatment, we obtained a profile of protection identical to that seen *in vivo* for leaf tissue: compare leaf lanes in Fig. 2 and DNase I data in Fig. 4 *A* and *C*. Hydroxyl radical cleavage confirms the wrapping of DNA around the histone octamer (Fig. 4 *B* and *C*). These results establish that positioning is dictated by the intrinsic sequence of the *phas* promoter. Although we have not yet determined the minimum sequence conferring the rotational position of the nucleosome, the region containing three phased TATA boxes is an attractive candidate. This notion is supported by computer analysis of the *phas* promoter sequence using a modified treatment of the program CURVATURE (33), which predicts the presence of sub-

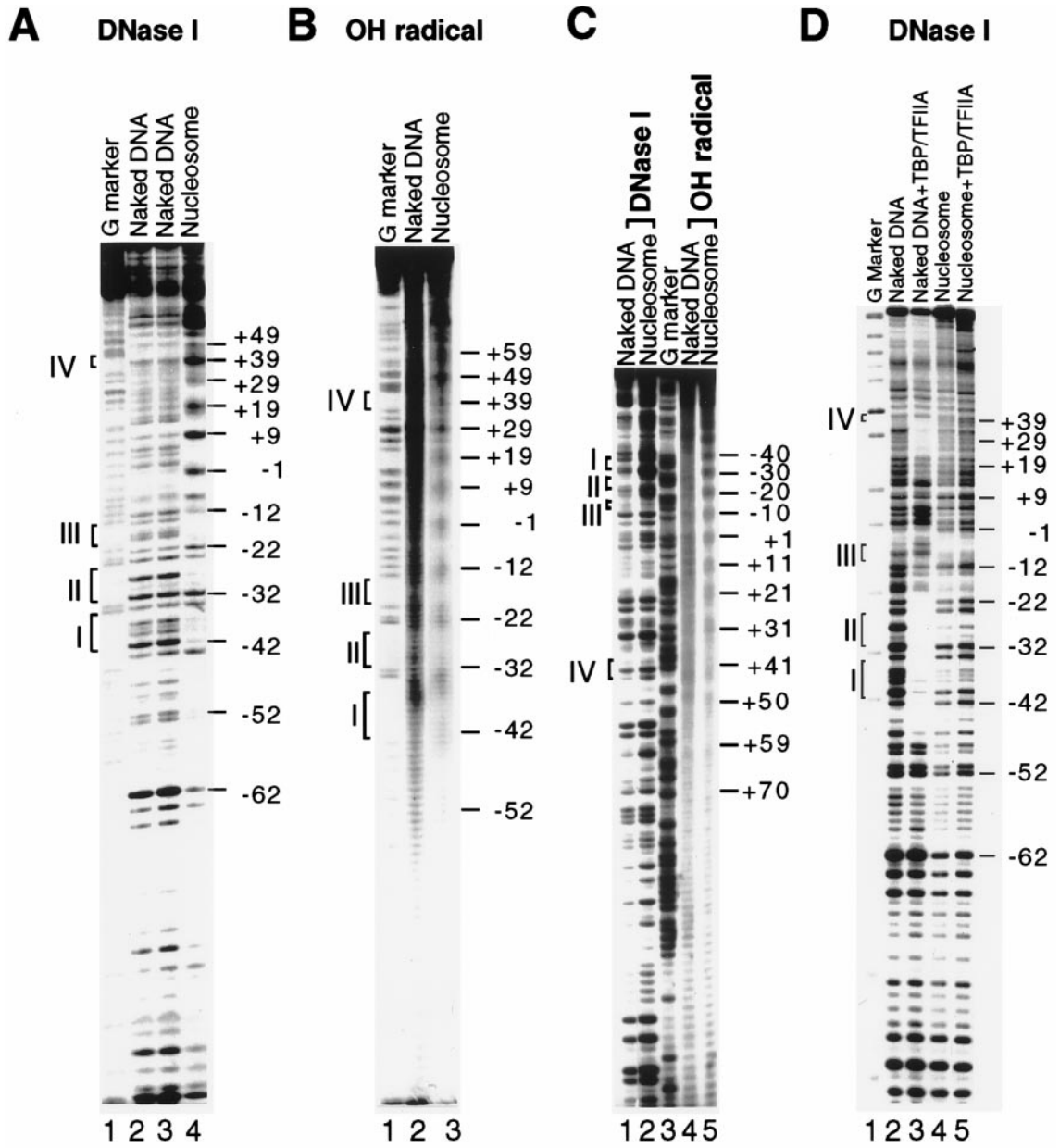

FIG. 4. Nucleosome reconstituted *in vitro* on a proximal fragment of the *phas* promoter and its effect on TBP binding. (*A*) DNase I footprinting of the bottom strand. For DNase I footprinting, the *Afl*III-*Xba*I fragment (−112 to +141) from the *phas* promoter in pBluescript II was reconstituted into nucleosomes and then treated with DNase I (1.5 units). After digestion, the nucleosome-bound fraction was separated by electrophoresis through a 0.7% agarose gel. The relevant band was electroeluted and run on a 6% denaturing acrylamide gel. (*B*) Hydroxyl radical footprinting of the bottom strand. Nucleosome reconstitution was as in *A*. For hydroxyl radical footprinting, cleavage was carried out by the generation of radicals through the Fenton reaction. Subsequent steps were as for DNase I footprinting. (*C*) DNase I and hydroxyl radical footprinting of the top strand of the *phas* proximal promoter. Footprinting was carried out as in *A* and *B*. (*D*) Incorporation of the *phas* promoter into a nucleosome prevents the binding of TBP. Equimolar amounts (400 nm) of TBP and TFIIA were added either to naked DNA (lane 3), or to reconstituted nucleosomes (lane 5), and binding was assessed by DNase I footprinting. For *A–D*, base positions are shown relative to the transcription start site. The *phas* TATA boxes, shown as brackets I to IV, are positioned at −41 to −35 (TATAATA), −32 to −25 (TATAAATA), −20 to −15 (TAATAT), and +37 to +43 (TATAATA).

stantial curvature in the TATA region, and by a recent evaluation of mouse genomic nucleosome-positioning sequences that has revealed that phased TATA boxes are among the strongest nucleosome-positioning signal yet characterized (34). Because chicken erythrocyte histone octamers were used for the *in vitro* nucleosome reconstitution experiments, another important implication of our results is that the mechanism of DNA–histone octamer interaction is highly conserved between plants and animals, probably reflecting the similarity of their H3 and H4 components (35).

The Rotationally Positioned Nucleosome Prevents Binding of TBP *in Vitro*. Each of the three TATA elements in the *phas* promoter is protected from DNase I cleavage *in vivo* by its orientation toward the surface of the histone core (Fig. 2); thus, the TATA boxes should be inaccessible to TBP. For nucleosome-free DNA, TBP bound *in vitro* to all three TATA boxes upstream of the *phas* promoter transcription start site (Fig. 4*D*), although binding to the TATA element closest to the transcription start site was at relatively low affinity. Another TATA element (TATAATA) exists downstream (+37 to +43) of the transcription start site. The function, if any, of this element is not clear, but it does not contribute to rotational positioning of the nucleosome because this is maintained on *phas* promoter elements lacking this region (data not shown).

In contrast to the binding of TBP to naked DNA, when the *phas* promoter fragment is incorporated into a nucleosome, no binding of TBP was detected for any of the four TATA elements (Fig. 4*D*). Earlier observations have shown that the incorporation of a TATA element into a nucleosome can prevent TBP binding even when the TATA element faces away from the histone core (27, 36). In the case of the *phas* promoter, the orientation of the TATA elements upstream of the *phas* promoter transcription start site toward the histone octamer presumably makes them totally inaccessible to TBP, in agreement with the absence of transcription from this promoter in vegetative tissues.

Translational Positioning May Contribute to the Rigorous Regulation of *phas* Expression. Variation in helical periodicity as revealed by hydroxyl radical cleavage (Fig. 4 *B* and *C*) suggested that the dyad region of the nucleosome approximates to the start site of transcription (37, 38). This translational positioning of the histone octamer was confirmed by micrococcal nuclease cleavage digestion followed by restriction endonuclease cleavage. As shown in Fig. 5, there are two preferred translational positions. One covers positions −74 to +72, and the other protects from −93 to +56. In either of these two positions, the TATA boxes, as well as the transcription start site, are protected by the nucleosome. These translational positions, if maintained *in vivo*, will also contribute to the complete lack of expression of the *phas* promoter in leaf tissues.

The Rotationally Positioned Nucleosome Is Replaced by TFIID During Transcription Activation. Three major alternatives exist for the observed differences in chromatin status between leaf and seed tissues: that the nucleosome present in transcriptionally inactive leaf tissues is remodeled (38–40), that it is shifted (41) (e.g., by sliding) to permit access by polymerase, or that it is completely displaced. Modification of nucleosomes on the *Xenopus* 5S RNA gene promoter by H2A and H2B removal or acetylation of the core histone tails does not significantly change the extent of protection from DNase I cleavage for a positioned nucleosome (38, 42), which is strikingly different from the shortening seen during transcriptional activation of the *phas* promoter (Fig. 2). Similarly, sliding of the nucleosome is an unsatisfactory explanation because it would not shorten the DNase I footprint. An alternative explanation for the short DNase I footprint on the *phas* promoter in seed nuclei (60 bp; Fig. 2*A*, −11 to +50) is that it represents the *phas* TATA region wrapped around the histone octamer-like substructure of TFIID (9–11). *In vitro* binding of purified TFIID to the *phas* promoter (Fig. 6) demonstrates that a modulated hydroxyl radical cleavage is obtained consistent with the DMS footprinting data. These observations are in accord with the findings for various promoters (12, 13, 43, 44) that purified TFIID makes contact at TATA boxes, the initiation site, and sites downstream of the transcription start site. Such binding of TBP to these sites would preclude binding of a nucleosome (27, 45). Our results are similar to the short 10-bp profile for DNase I footprints seen for the *Ad2ML* promoter when bound by TFIID (12, 13) and suggest that the histone octamer is displaced and replaced by TFIID.

The results shown here, using a combination of *in vivo* and *in vitro* approaches, reveal that the proximal region of the *phas* promoter can rotationally position a nucleosome over sequences that include three phased TATA motifs and the transcription initiator. The chromatin structure endowed by this precise positioning probably is responsible for correct regulation of *phas* gene expression and may be crucial for the complete lack of expression in vegetative tissues. Indeed, a nucleosome located in the vicinity of the RNA start site has been shown to completely inhibit TBP binding to the adenovirus major late promoter and to block RNA polymerase II transcription *in vitro* from the *Drosophila Krüppel* promoter (36, 46). The well studied promoters of mouse MMTV, yeast PHO5, and *Xenopus* 5S RNA genes each have a nucleosome positioned over the transcription start site that has been implicated in regulating expression (37, 47–49). A crucial function of

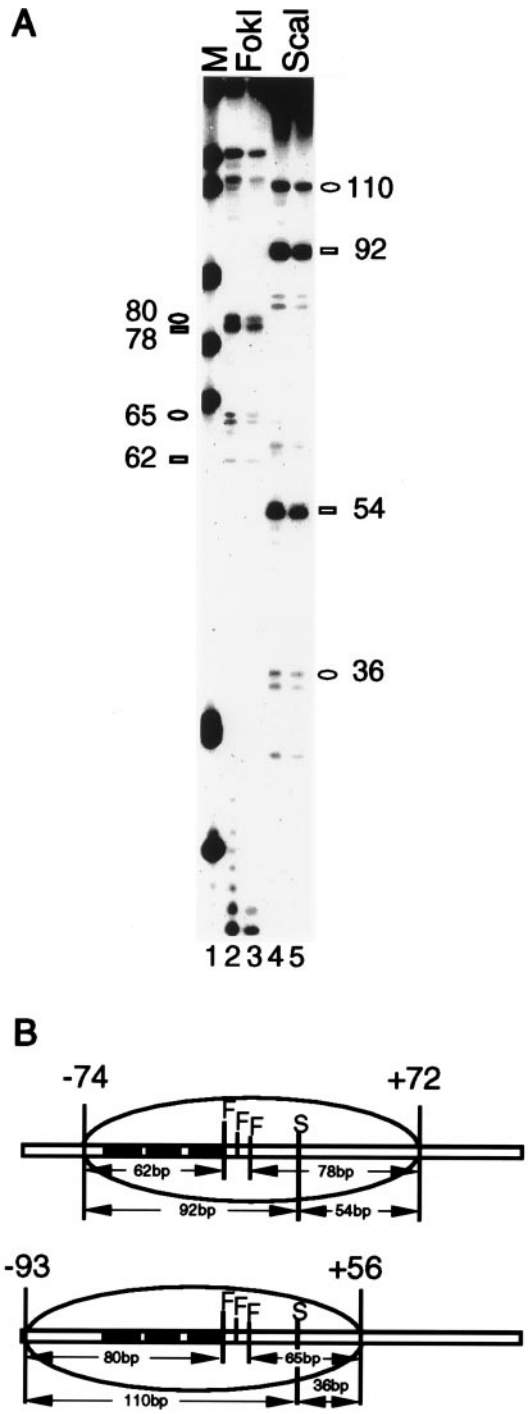

FIG. 5. Translational mapping of the nucleosome on the *phas* promoter. The *Afl*III-*Xba*I fragment (−112 to +141) from the *phas* promoter in pBluescript II was reconstituted into nucleosome. The resultant nucleosomal complex was treated with micrococcal nuclease (0.07 units), and the kinase-labeled products were loaded onto a 6% native polyacrylamide gel. The relevant band was excised and eluted. The DNA was then extracted with phenol and cleaved with either *Fok*I or *Sca*I, and the products were separated on a 6% denaturing gel. (*A*) Two major translational settings were revealed. The *Fok*I (lanes 2 and 3) or *Sca*I (lanes 4 and 5) fragment positions are denoted by a rectangle (for the −74/+72 setting) or an oval (for the −93/+56 setting). Lane 1 is a marker (M) lane containing *Msp*I-digested pBR322. (*B*) Diagram of the two major translational positions. Solid rectangles denote TATA boxes. Restriction enzyme sites: F, *Fok*I; S, *Sca*I.

the α2 repressor in silencing the yeast chromosomal α-mating type-specific gene *in vivo* is to cause a nucleosome to be positioned over the TATA box (50). Thus, it appears that repression

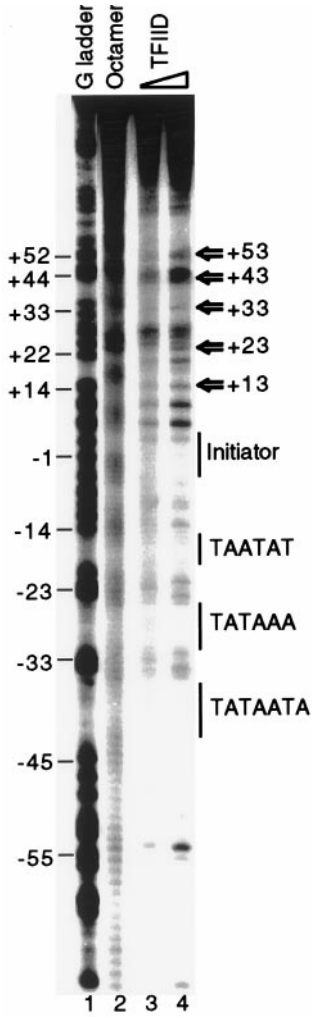

FIG. 6. Hydroxyl radical footprinting of the complex of TFIID with the *phas* promoter. Lane 1, G ladder with positions shown relative to the transcription start site; lane 2, cleavage of the *phas* fragment in a reconstituted nucleosome; lanes 3 and 4, cleavage of the fragment bound by 200 ng or 300 ng of TFIID, respectively.

of basal transcription by situating a nucleosome over the TATA region is a mechanism employed by many promoters. The *phas* example is unique in that the rotational placement of the nucleosome protects a series of three phased TATA motifs and the transcription start site. This makes it an ideal system to study the exchange between the nucleosome and TFIID during the architectural transition from an inactive domain to an active transcriptional complex.

We thank Apolonia van der Geest, Mahesh Chandrasekharan, Mark Guiltinan, and lab members for discussions and suggestions. This work is supported by National Science Foundation Grant MCB-9604617 to T.C.H. S.P.C. is the recipient of a Wellcome Trust International Prize Traveling Fellowship.

1. Grunstein, M. (1990) *Annu. Rev. Cell Biol.* **6,** 643–678.
2. Simpson, R. T. (1991) *Nucleic Acids Res. Mol. Biol.* **40,** 143–184.
3. Felsenfeld, G. (1992) *Nature (London)* **355,** 219–224.
4. Owen-Hughes, T. & Workman J. W. (1994) *Crit. Rev. Eukaryotic Gene Expression* **4,** 403–441.
5. Schild, C., Claret, F.-X., Wahli, W. & Wolffe, A. P. (1993) *EMBO J.* **12,** 423–433.
6. Lu, Q., Wallrath, L. L., Granok, H. & Elgin, S. C. R. (1993) *Mol. Cell. Biol.* **13,** 2802–2841.
7. van Holde, K. E. & Zlatanova, J. (1996) *BioEssays* **18,** 697–700.
8. Hoffman, A., Oelgeschläger, T. & Roeder, R. G. (1997) *Proc. Natl. Acad. Sci. USA* **94,** 8928–8935.
9. Hoffman, A., Chiang, C.-M., Oelgeschläger, T., Xie, X., Burley, S. K., Nakatani, Y. & Roeder, R. G. (1996) *Nature (London)* **180,** 356–359.
10. Nakatani, Y., Bagby, S. & Ikura, M. (1996) *J. Biol. Chem.* **271,** 6575–6578.
11. Xie, X., Kokubo, T., Mirza, U. A., Hoffmann, A., Chait, B. T., Roeder R. G., Nakatani, Y. & Burley, S. K. (1996) *Nature (London)* **380,** 316–322.
12. Sawadogo, M. & Roeder, R. G. (1985) *Cell* **43,** 165–175.
13. Oelgeschläger, T., Chiang, C.-M. & Roeder, R. G. (1996) *Nature (London)* **382,** 735–738.
14. Van Holde, K. E. (1988) *Chromatin* (Springer, New York).
15. Sun, S. M., Mutschler, M. A. Bliss, F. A. & Hall, T. C. (1978) *Plant Physiol.* **61,** 918–923.
16. Sengupta-Gopalan, C., Reichert, N. A., Baker, R. F., Hall, T. C. & Kemp, J. D. (1985) *Proc. Natl. Acad. Sci. USA* **82,** 3322–3324.
17. van der Geest, A. H. M., Hall, G. E., Spiker, S. & Hall, T. C. (1994) *Plant J.* **6,** 413–423.
18. van der Geest, A. H. M., Frisch, D. A., Kemp, J. D. & Hall, T. C. (1995) *Plant Physiol.* **109,** 1151–1158.
19. Frisch, D. A., van der Geest, A. H. M., Dias, K. & Hall, T. C. (1995) *Plant J.* **7,** 503–512.
20. Hall, G., Jr., Allen, G. C., Loer, D. S., Thompson, W. F. & Spiker, S. (1991) *Proc. Natl. Acad. Sci. USA* **88,** 9320–9324.
21. Ingelbrecht, I. & de Carvalho, F. (1992) in *EMBO Practical Course on Plant Molecular Biology,* eds. Inzé, D., Van der Straeten, D. & Van Montagu, M. (Laboratorium voor Genetica, Gent, Belgium), pp. 117–132.
22. Mueller, P. R. & Wold, B. (1989) *Science* **246,** 780–786.
23. Simon, R. & Felsenfeld, G. (1979) *Nucleic Acids Res.* **6,** 689–696.
24. Camerini-Otero R., Sollner-Webb, B. & Felsenfeld, G. (1976) *Cell* **8,** 333–347.
25. Hayes, J. J. & Wolffe, A. P. (1993) *Proc. Natl. Acad. Sci. USA* **90,** 6415–6419.
26. Tatchell, K. & van Holde, K. E. (1977) *Biochemistry* **16,** 5295–5303.
27. Godde, J. S., Nakatani, Y. & Wolffe, A. P. (1995) *Nucleic Acids Res.* **23,** 4557–4564.
28. Ge, H., Martinez, E., Chiang, C.-M. & Roeder, R. G. (1996) *Methods Enzymol.* **274,** 57–71.
29. Imhof, A., Yang X.-J., Ogryzko, V. V., Nakatani, Y., Wolffe, A. P. & Ge, H. (1997) *Curr. Biol.* **7,** 689–692.
30. Wolffe, A. P. & Hayes, J. J. (1993) *Methods Mol. Genet.* **2,** 314–330.
31. Tullius, T. D., Dombroski, B. A., Churchill, M. E. A. & Kam, L. (1987) *Methods Enzymol.* **155,** 537–558.
32. Lutter, L. C. (1978) *J. Mol. Biol.* **124,** 391–420.
33. Shpigelman, E. S., Trifonov, E. N. & Bolshoy, A. (1993) *CABIOS* **9,** 435–440.
34. Widlund, H. R., Cao, H., Simonsson, S., Magnusson, E., Simonsson, T., Nielsen, P. E., Kahn, J. D., Crothers, D. M. & Kubista, M. (1997) *J. Mol. Biol.* **267,** 807–817.
35. Chabouté, M. E., Chaubet, N., Gigot, C. & Philipps, G. (1993) *Biochimie* **75,** 523–531.
36. Imbalzano, A. N., Kwon, H., Green, M. R. & Kingston, R. E. (1994) *Nature (London)* **370,** 481–485.
37. Hayes, J. J., Tullius, T. D. & Wolffe, A. P. (1990) *Proc. Natl. Acad. Sci. USA* **87,** 7405–7409.
38. Hayes, J. J., Clark, D. J. & Wolffe, A. P. (1991) *Proc. Natl. Acad. Sci. USA* **88,** 6829–6833.
39. Truss, M., Bartsch, J., Schelbert, A., Haché, R. J. G. & Beato, M. (1996) *EMBO J.* **14,** 1737–1751.
40. Vega-Palas, M. A. & Ferl, R. J. (1995) *Plant Cell* **7,** 1923–1932.
41. Varga-Weisz, P. D., Blank, T. A. & Becker, P. B. (1995) *EMBO J.* **14,** 2209–2216.
42. Lee, D. Y., Hayes, J. J., Pruss, D. & Wolffe, A. P. (1993) *Cell* **72,** 73–84.
43. Purnell, B. A., Emanuel, P. A. & Gilmour, D. S. (1994) *Genes Dev.* **8,** 830–842.
44. Weber, J. A. & Gilmour, D. S. (1995) *Nucleic Acids Res.* **23,** 3327–3334.
45. Workman, J. L. & Roeder, R. G. (1987) *Cell* **51,** 613–622.
46. Laybourn, P. J. & Kadonaga, J. T. (1991) *Science* **254,** 238–245.
47. Richard-Foy, H. & Hager, G. L. (1987) *EMBO J.* **6,** 2321–2328.
48. Straka, C. & Hörz, W. (1991) *EMBO J.* **10,** 361–368.
49. Rhodes, D. (1985) *EMBO J.* **4,** 3473–3482.
50. Shimizu, M., Roth, S. Y., Szent-Gyorgi, C. & Simpson R. T. (1991) *EMBO J.* **10,** 3033–3041.